MONOCRYSTALLINE STRUCTURE FORMATION OF DOPED PERFECT SILICON CRYSTALS

N.A. Azarenkov[1], V.E. Semenenko[1], A.I. Ovcharenko[1], M.M. Pylypenko[2]
[1] V.N. Karazin Kharkiv National University, Kharkov, Ukraine;
[2]National Science Center “Kharkov Institute of Physics and Technology”, Kharkov, Ukraine

In this paper we consider perfect doped silicon single crystals growth. Special features of anodic etching of n- and p-type single crystals has been revealed. An impact of seed orientation on dislocation and defect structure evolution in crystal on different growth stages has been found. Influence of heat treatment on phase-structural condition of single crystals and nonequilibrium carrier lifetime has been determined.

PACS:81.10.Fq, 88.40.jj, 78.40.Fy, 81.40.-z, 85.40.Ry, 72.10.Fk

INTRODUCTION

One of the main tasks of modern material science – development and research of new structural materials with controlled structure and stable physical and mechanical properties. A problem of today is search and improvement of new renewable sources of energy, share of which is about to increase by 40% until 2040 in the overall energy balance in European Union [1, 2].

High-purity silicon crystals and their solid solutions are widely used in solid state electronics to create sensors of physical quantities, optoelectronics, nanoelectromechanical systems etc. [3–5]. Efficiency of amorphous, polycrystalline and single-crystalline silicon based solar cells is ~ 10, ~ 18.5, 25%, respectively [1, 6]. Theoretically, the maximum efficiency of GaAs solar cells is ~ 33.5% (AM 1.5G, Shockley-Queisser limit). Due to high efficiency and low degradation after being exposed to space radiation, they prevail in space industry [7, 8]. In the latter case, heterophase converter AlGaAs-GaAs structures are implied. Despite the creation of different types of solar cells, naturally widespread silicon (amorphous, polycrystalline, single-crystalline and nanostructured) keeps making up an essential part of their worldwide production. Currently physical mechanisms of charge carriers scattering in semiconductors – scattering by neutral and ionizing impurities, grain boundaries, acoustic phonons, polar and non-polar optical phonons, mutual scattering of mobile carriers [4, 9, 10] are being widely studied. Many authors point out degradation of solar cells properties. Determination of the causes of thermal instability and electrical properties of doped silicon single crystals is exaggerated by the fact that when heated to high temperatures, various physical processes become intertwined. Actual data suggests that the main cause of minority carrier lifetime variation are diffusion processes in semiconductor materials. It is clear that in order to understand thermal instability of semiconductors after heat treatment (HT), scattering mechanisms in single crystals of semiconductors and achieve effective efficiency improvement, information about the influence of impurity composition and phase structure, structural micro- and macroscopic defects on their physical and mechanical properties’ stability is required. However, these physical phenomena are not studied sufficiently [5, 10–15]. It should be noted, that most studies specify the use of dislocation-free silicon crystals. At the same time it is known that the most perfect crystals are whiskers that are grown in special molecular kinetic growth conditions, their dislocation density is $< 10^1…10^2$ cm^{-2} [16, 17].

The aim of this work is to grow perfect doped silicon single crystals, study the evolution of dislocation structure in crystals that are being grown in different molecular-kinetic conditions and its influence on minority carrier lifetime.

EXPERIMENTAL

The study was performed on the samples of polycrystalline purified (99.99%) and solar grade Si (99.999%), donor impurity – phosphorus ($4.5\cdot10^{16}$ cm^{-3}), acceptor impurity – boron ($1.3\cdot10^{17}$ cm^{-3}), which form limited substitutional solutions [18, 19].

In order to achieve homogenization of the alloy, ingots were melted in an inert atmosphere, growth from the melt was performed with positive temperature gradient using oriented crystallization (Czochralski method, vacuum $< 10^{-4}$ Pa, crystallization rate $R = 1\cdot10^{-5}…3\cdot10^{-5}$ m/s, temperature gradient on the liquid-solid phase border G ~ 50…100 K/cm). n- and p-type silicon single crystals resistivity ~ 0.001…200 Ω·cm. Metallographic, X-ray crystal (DRON 4M) and electron microscopic analyses (UEM-100 K, Tesla BS-163 with accelerating voltage of 80 kV).

Beforehand silicon wafers were thinned using one-side chemical polishing technique with HNO_3:HF:CH_3COOH = 3:1:1. Samples were subjected to anodic etching in the mix of acids HF(48%):HNO_3(52%) = 10:15 during 10…15 s. Dislocation density was determined with the help of etch pits and transmission electron microscopy (TEM) similarly to [16]. Dislocation decoration with Cu was observed in crystals that were beforehand covered with a layer of cuprum nitrate with subsequent heating in hydrogen. Conductivity type was determined using thermoprobe and voltage-current characteristic. Resistivity – using two- and four-probe method. Nonequilibrium carrier lifetime was determined using photoconductive decay method. Dopant concentration – using mass spectroscopy and activation analyses.

RESULTS AND DISCUSSION

Different nature of n- and p-type semiconductors’ etching, which is due to their electrochemical behavior in electrolyte solutions, was revealed. It is known that in metals, electric charge is concentrated in the surface

layer of the depth of 10^{-8} cm. In semiconductors, depth of volume charge layer depends on the carrier quantity and can be up to $10^{-5}…10^{-4}$ cm. Therefore, during double electrical layer formation on the semiconductor surface in electrolyte solution, diffusion lining can appear both from solution and semiconductor sides. In p-type crystals, where holes are majority carriers, comparatively small concentration of free carriers affects the makeup of the double electrical layer on the semiconductor-solution interface. Anodic process undergoes easily and does not differ from the similar process for metallic samples. In n-type crystals, where holes are minority carriers, anodic etching rate is determined by the rate of holes coming to the electrode surface. Optimal etching rates have been determined:

Si samples	n-type	p-type
Current density, mA/cm^2	15…20	50…60
Etching time τ, min	5…7	10…12

It should be noted that the combination of anodic and chemical etching in the etchant with chrome anhydride allows investigating impurity distribution in the volume of silicon single crystals in a wide range of resistivities.

Metallographic analysis of Si single crystals (99.99%) that were grown from the melt using oriented crystallization method, shows that observed spiral crystal growth agrees with traits of external surface of the crystal similar to Fig. 1. During metallographic examinations, striations in silicon single crystals were observed. It is inherent in the growth process and are, probably, associated with some periodic change in impurities' concentration right by the crystallization front (see Fig. 1,b). It should be noted that similar striations were not observed in crystals based on high-purity silicon.

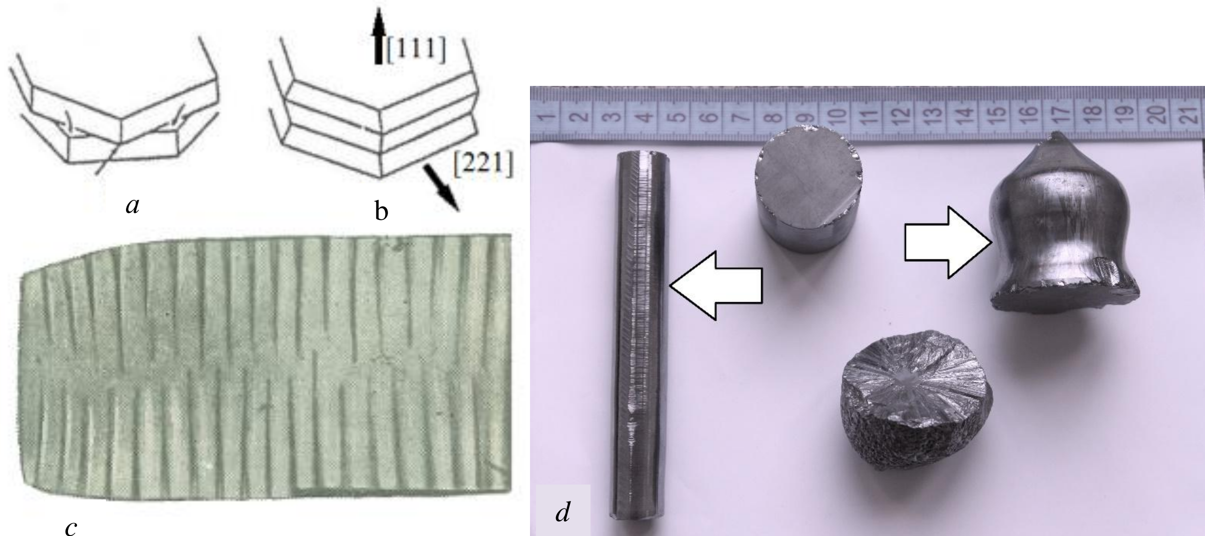

Fig. 1. Mechanisms of crystal growth:
a – growth step formation; b – step, caused by diamond structure twinning;
c – growth bands (cross-section, x2); d – silicon single crystals (indicated with an arrow)

It should be noted that an analogy is observed between purification that occurs during Czochralski process and floating-zone refining method [20]. Impurity distribution in growing crystal is determined by an effective distribution coefficient [16]:

$$k_{ef} = \frac{k}{k + (1-k)\exp\left(-\frac{R}{D_{liq}}\right)}, \quad (1)$$

where k is the equilibrium distribution coefficient; R – linear rate of crystallization, cm/s; δ – diffusion layer thickness, cm; D_{liq} – dopant diffusion coefficient in the melt, cm^2/s. Diffusion layer thickness that is present in (1), can be found form an empirical dependence: $\delta = 1.6 D_{liq}^{1/3} \nu^{1/6} \omega^{-1/2}$, where ω – crystal rotation rate, s^{-1}; ν – kinematic viscosity of the melt, cm^2/s. Distribution coefficients of the main impurities in silicon are the following: P – 0.35, B – 0.8; C – $7\cdot10^{-2}$; O – 1.25; Al – $2\cdot10^{-3}$; Cu – 10^{-4}; As – 0.3; W – $5\cdot10^{-8}$. It is determined that the most effective refinement during oriented crystallization is observed for Zr, Mo, W, Ta, Nb, Cd, Bi. Rather effective is Ti, V, Cr, Mn, Fe, Co, Zn, Ni, Cu, Ga, Ag refinement.

Silicon nitride crucibles, used in this study instead of common quartz ones, and tungsten heaters (instead of graphite ones) allowed to reduce the content of "harmful" impurities – oxygen, carbon and nitrogen, significantly. Oxygen concentration was $2\cdot10^{15}…2\cdot10^{16}$ cm^{-3} ($2.29\cdot10^{-6}…2.29\cdot10^{-7}$ wt.%), carbon and nitrogen ~ 10^{16} cm^{-3} (~ 10^{-5} wt.%).

In order to determine the mechanism of silicon single crystals growth, differently oriented monocrystalline seeds were used. Fig. 2,a shows the behavior of single crystal structure formation from a polycrystalline seed. As can be seen, polycrystal forms because primitive crystals' of different orientation collisions and their subsequent selective growth. At the same time microdistortions of the growing crystal appear. They are caused by linear and point defects, grain boundaries, dislocated atoms etc. Usually, dislocation density of polycrystals is ~ $10^5…10^8$ cm^{-2}.

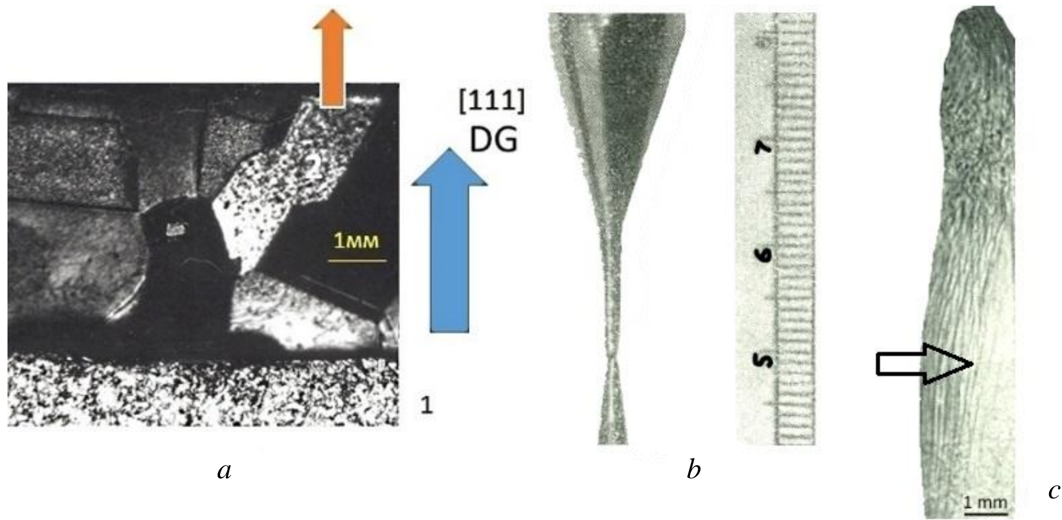

a *b* *c*

Fig. 2. Silicon monocrystalline structure formation:
a – crystal selective growth (arrow indicates direction of grows, GD);
b – shape of growing crystal;
c – dislocation structure, dislocations are indicated with an arrow

It has been determined that when monocrystalline oriented seed is used, crystal grade greatly depends on the initial conditions of the growth, when overheating of the melt is required for ensuring an ingot with small diameter and optimal conditions for dislocations to reach the surface. After several diameters long “pinch-neck” formation, epitaxy of the crystal from the size of the neck to the ingot’s nominal diameter was carried out (see Fig. 2,c). In what follows, growth conditions are stabilized in order to get an ingot with fixed diameter (~ 20…30 mm) and high structural perfection (see Fig. 1,d). On this stage, thermal conditions define temperature gradient G, shape of the crystallization front and size of the undercooled region nearby. In order to prevent a non-uniform impurities distribution in the growing crystal, the crucible with the melt was placed in a magnetic field that slows the motion of the conductive melt. Magnetic viscosity effect – an increase of melt viscosity in the magnetic field to a value that exceeds its own kinematic viscosity is being observed [21].

The effect of different seed orientations ([111], [110], [112] and [100]) on crystal perfection was determined. Electron microscopic analysis of the crystals shows that there are dislocations on early stages of growth. The number of dislocations that were formed by the plastic flow depends on thermal stresses on the phase interface. Presence of temperature gradient in growing crystal (at a fixed growth rate) causes its oversaturation with vacancies; they “freeze” in solid phase. According to calculations, vacancy equilibrium concentration in silicon at room temperature is $10^7…10^8$ cm^{-3}, at 1000 °C it raises up to $10^{17}…10^{18}$ cm^{-3}. As a result, oversaturation with vacancies can cause dislocation climb or their condensation in aggregates. It has been determined that during the process of controlled phase transformation vacancies oversaturation favors the climb of vacancies with edge components, that can leave the crystal. In crystals that grow in the [110] direction, there are long unbent dislocations parallel to the growing axis. As it has been found, in cuprum decorated crystals many of such dislocations have screw orientation (Fig. 3,a).

According to TEM, helicoids have formed on screw dislocations. As can be seen from Fig. 3,a, dislocations form tight helices parallel to [110]. The arrow indicates prismatic loops that were formed, probably, by a glide dislocation (see Fig. 3,b). Formation of dislocation loops may be caused by the recombination of interstitial boron atoms with thermally activated vacancies [22]. Big loops parallel to {111} plane, probably, have a different origin. As it has been determined, loop regions are stacking faults surrounded by partial dislocations. Big loops have a diameter of ~ 50 μm. Electron microscopic analysis shows that abundance of point defects, that emerges in the crystal during liquid-solid phase transition, tends to hold screw dislocation parallel to its Burgers vector. As a result, it can stretch out for a long distance without being distorted. It should be noted that crystal growth in [110] direction has a flaw that leads to screw dislocations parallel to this direction not being removed with the climb. Dislocation density in such crystals is $10^3…10^4$ cm^{-2}. However, if the growing axis is not parallel to a Burgers vector, screw dislocation is usually pushed out to the surface.

Thus, the most perfect crystals are obtained when [111] and [100] oriented seeds are used, $\rho_d \le 3…5\cdot10^2$ cm^{-2}, static temperature gradient G = 40…85 K/cm. The latter is explained by the fact that in the samples with [100] growing axis rectilinear dislocations 10 cm long (see Fig. 2,c) were found. These dislocations continue to exist in conditions favorable to their climb; Burgers vector b = [100]. At the same time in crystals with [110] and [112] growing axes, that were grown in conditions favorable to oversaturation with vacancies, primary dislocation alignment parallel to growing axis was not detected. Their dislocation density is $10^3…10^4$ cm^{-2}.

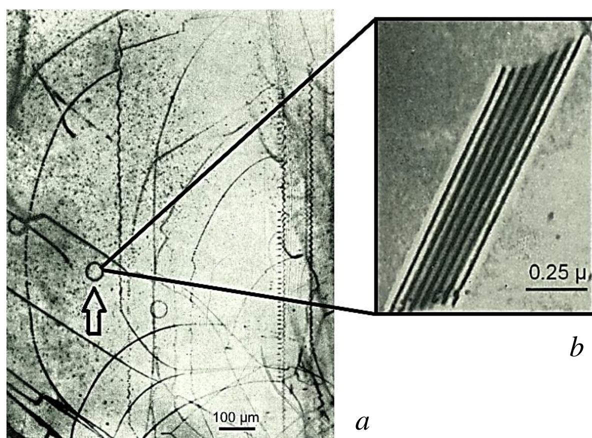

Fig. 3. Silicon single crystals microstructure: a – dislocation structure of crystals that were grown using [110] oriented seed; b – stacking faults

With the help of metallurgical and electron microscope studies it was found that during semiconductor solid solutions growth, when one grain solidifies as a pure crystal and impurity atoms are displaced outwards, impurity concentration ~ 1 ppm (P – $1.1 \cdot 10^{-6}$ wt.%, B – $3.86 \cdot 10^{-7}$ wt.%), is sufficient to cover all grain boundaries with an atomic layer of impurity. In our study in doped n- and p-type crystals phosphorus and boron concentration was 0.9 and 2.6 ppm, respectively. In pure crystals (99.95%) local concentration of impurity that is located on grain boundaries is feasible. Such a segregation means that crystal properties are not identical in the bulk of a crystal. According to refs 10 and 23, atom clusters can cause local lattice bending, leading to a structure that is similar to "hereditary" which is observed in metallic crystals (Fig. 4). Such deformations are likely to affect photoelectric properties of solar cells (Fig. 5,b).

Influence of HT on nonequilibrium carrier lifetime was investigated using grown silicon crystals of different degree of structure perfection. So far, the existence of phase structural semiconductors' composition, HT processes and electrophysical properties relation remains uncertain. In order to reveal the influence of impurity diffusion from silicon crystals surface on minority carrier lifetime τ during HT (spectroscopically pure helium atmosphere, 800 °C, 30 min, cooling rate ~ 100 deg/min), silicon n-type monocrystals (resistivity ρ = 4.5…5 Ω·cm) were studied. Puck-shaped samples with different thickness, meaning different surface area, were used. Oxygen concentration was ~ $5 \cdot 10^{17}$ cm^{-3}. In order for the surface recombination not to overlap HT influence on τ, relative change of the τ value was measured in respect to volume to surface ratio V/S (see Fig. 5,a).

As can be seen from Fig. 5,a, shapes of the two curves are roughly the same. Carrier lifetime decrease under HT due to the increase of specific surface of a sample is, probably, caused by recombination centers diffusion from its surface.

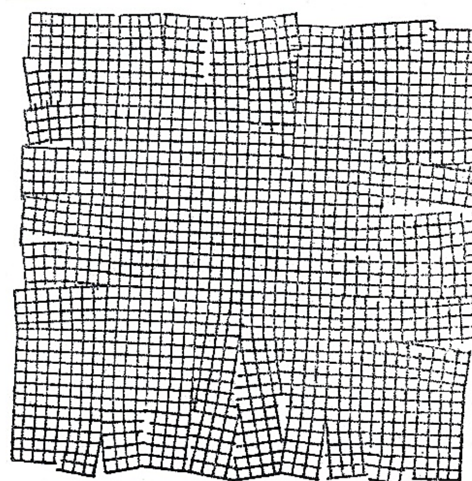

Fig. 4. Diagrammatic representation of "hereditary" structure

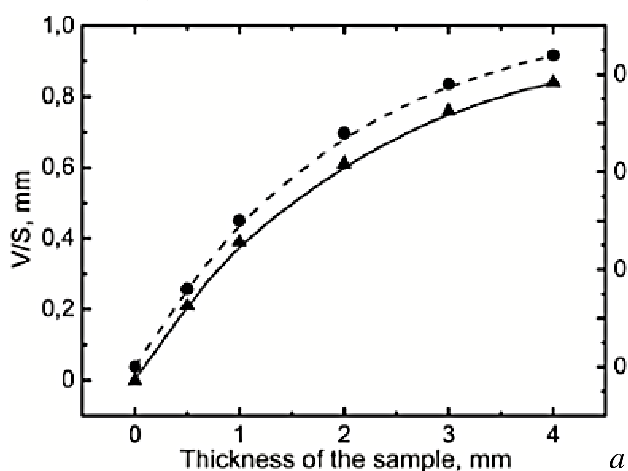

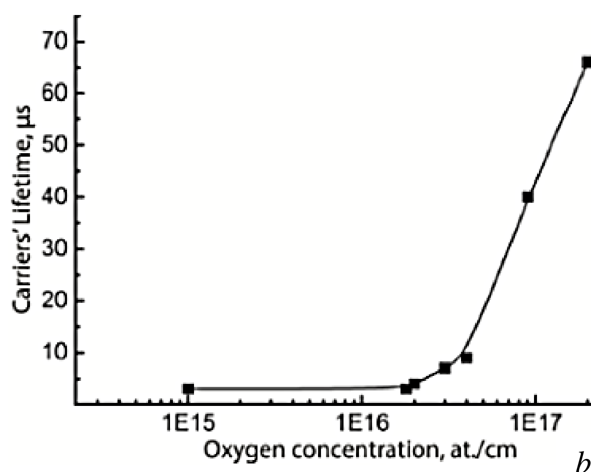

Fig. 5. Relative minority carrier lifetime (τ/τ_0) (1) and V/S (2) as functions of samples' thickness, HT at 800 °C (a); minority carrier lifetime in silicon after HT at 800 °C as a function of oxygen leaving the solid solution (b)

For the purpose of studying changes of τ value in silicon single crystals of electron and hole conduction type (ρ = 50 and 300 Ω·cm), depending on their oxygen content, 3x6x15 mm samples that were cut perpendicular to [111] direction, has been considered. Heat treatment was performed in vacuum <10^{-3} Pa, at 800 °C for 30 min, heating rate – 200 deg/min, cooling – 40. As can be seen from Fig. 5,b and Table 1, the

more oxygen is leaving the solid solution (maximum oxygen solubility in silicon at 1400 °C – 10^{18} cm^{-3} (~ 1.1·10^{-3} wt.%), at 1000 °C ~ 2·10^{16} cm^{-3} (~ 2.3·10^{-5} wt.%) and rapidly declining with temperature decrease), the bigger the value of residual minority carrier lifetime [18]. It was found that recombination centers appear in the bulk of silicon single crystals during HT mainly because of impurities from the outside. At the same time they are neutralized by oxygen that leaves the solid solution forming complexes that contain electrically active impurities (boron, aluminum) [22, 24]. At high temperatures fracture of the complexes is observed, recombination activity of the centers increases.

Table 1

Oxygen concentration in solid solution and minority carrier lifetime variation, HT at 800 °C, 30 min

Properties before HT		Properties after HT		
Lifetime, microseconds	The content of oxygen, at./cm^3	Lifetime, microseconds	The content of oxygen, at./cm^3	The concentration of oxygen leaving the solid solution, at./cm^3
n-type conductivity				
100	3·10^{16}	<3	3·10^{16}	0
30	5·10^{16}	<3	4.9·10^{16}	0.1·10^{16}
180	7.2·10^{16}	<3	5.4·10^{16}	1.8·10^{16}
55	9.6·10^{16}	6	8.8·10^{16}	0.8·10^{16}
40	1.3·10^{17}	9	9·10^{16}	4·10^{16}
87	4·10^{17}	45	–	–
90	5·10^{17}	66	3·10^{17}	20·10^{16}
n-type conductivity				
30	5.6·10^{16}	4	3.6·10^{17}	2·10^{16}
60	9.7·10^{16}	7	6.7·10^{16}	3·10^{16}
54	2.6·10^{17}	40	1.7·10^{16}	9·10^{16}
85	2.7·10^{17}	35	1.5·10^{16}	1.2·10^{16}
78	6.1·10^{17}	42	–	–

Minority carrier lifetime of doped silicon single crystals subjected to HT was determined. As can be seen from Table 2, under a high-temperature anneal (up to 1200 °C), difference in dislocation density (10^2…5·10^4 cm^{-2}) does not influence the value of τ after HT – in every case it is < 3 µs. Contrary to this, when heated up to 800 °C, similar samples show different τ for each value of dislocation density. In crystals with $\rho_d < 10^2$ cm^{-2} τ virtually did not change after HT, while in crystals with $\rho_D \sim 10^2$ cm^{-2} it decreased by a factor of 8.

Table 2

Influence of heat treatment on electrical properties of silicon

Properties before HT			Properties after HT	
The dislocation density , cm^{-2}	ρ, Ω·cm	τ, µs	ρ, Ω·cm	τ, µs
At 800 °C				
5·10^4	10.8	39	12.9	5
2.3·10^4	11.9	37.4	13.1	4.6
4.5·10^4	13.7	37	13.6	5.4
<10^2	54	19	60.5	18
<10^2	67	20	49	15
<10^2	70	17	65.4	16
At 1200 °C				
>10^4	12.3	27	12	<3
5·10^4	11.9	23	15.4	<3
3·10^4	12.4	27	13.4	<3
<10^2	51.0	23	66.6	<3
<10^2	68.0	39	64	<3
<10^2	56.5	21	70.1	<3

The latter is probably caused by the increase of dislocation diffusion contribution, which rate is ~10^6…10^7 times bigger than bulk and grain boundary diffusion rate [12, 24]. Moreover, dislocations cause hydrostatic stresses that lead to deformation of energy band. With the increase of dislocation density, band gap decreases [10]. Thus, the change in the band gap magnitude and increased diffusion permeability in

single crystals with high dislocation density ($10^3…10^4$ cm^{-2}) cause a significant change of nonequilibrium carrier lifetime.

CONCLUSIONS

Doped silicon single crystals with various dislocation densities have been grown using oriented crystallization method. Spiral growth of silicon monocrystals was detected. It agrees with crystal outer surface structural feature. Characteristic properties of doped monocrystals anodic etching have been determined. They are due to the influence of charge carriers on the structure of double electrical layer on the semiconductor-melt layer.

The influence of seed orientation on the formation kinetics of single crystal structure has been determined. At the early stages of growth, formation of dislocation and regions, supersaturated with vacancies, lead to dislocation climb or their condensation into aggregates. The most perfect monocrystals ($\rho_d \sim 3…5\cdot10^2$ cm^{-2}) were grown using [111] and [100] oriented seeds, static temperature gradient ~ 40…85 K/cm.

Influence of heat treatment on minority carrier lifetime has been determined. In crystals with $\rho_d \sim 10^3…10^4$ cm^{-2}, τ decreased by a factor of 8 (from 39 to 5 μs). This is due to dislocations that cause a band gap change and an increased diffusion permeability of the samples. It was shown that in silicon single crystals with low dislocation density ($\rho_d < 10^2$ cm^{-2}) the value of τ is virtually unchanged.

Obtained results can be applied for choosing a heat treatment rate and producing semiconductor materials of various purity that have a stable structure and electrophysical properties.

REFERENCES

1. В.А. Шаповалов. Солнечный кремний // *ВАНТ. Серия «Вакуум, чистые материалы, сверхпроводники».* 2014, №1(89), с. 53-55.
2. K. Chang. *Solar cells and their applications*, 2nd ed. Part II, VI – John Wiley & Sons, 2010, 644 p.
3. O. Schultz, S. Glunz, S. Riepe, et al. High-efficiency solar cells on phosphorus gettered multicrystalline silicon subtracts // *Prog. Photovolt: Res. Appl*. 2006, v. 14(8), p. 711-719.
4. *Report Citation REN 21.2011. Renewables 2011 Global status report.* Paris: REN21 Secretariat, 2011, 116 p.
5. S. Liu, X. Niu, W. Shan, et al. Improvement of conversion efficiency of multicrystalline silicon solar cells by incorporating reactive ion etching texturing // *Sol. Energ. Mat. Sol. Cells.* 2014, v. 127, p. 21-26.
6. L.D.A Jouini, N. Plassat, D. Ponthenier, et. al. *Proc. 5th International Workshop on the Crystalline Silicon Solar Cells*, Boston, 2011.
7. M. Yamaguchi. Radiation-resistant solar cells for space use // *Sol. Energ. Mat. Sol. Cells.* 2001, v. 68, issue 1, p. 31-53.
8. B.E. Anspaugh. *GaAs solar cell radiation handbook.* V. 1. *National Aeronautics and Space Administration, Jet Propulsion Laboratory*, California Institute of Technology, 1996.
9. Ю.А. Загоруйко, В.М. Пузиков, О.А. Федоренко, Н.О. Коваленко. *Модификация физических свойств широкозонных полупроводников $A^{II}B^{VI}$.* Харьков: Ин-т монокристаллов, 2005, 351 с.
10. A.M. Kosevich. *The Crystal Lattice. Phonons, Solitons, Dislocations, Superlattices*, “WILEY-VCH”, Weinheim, 2005, 345 c.
11. A.A. Druzhinin, I.P. Ostrovsky, Y.N. Hoverko et al. Silicon Whiskers Preparation // *Nanosystems, nanomaterials, nanotechnology.* 2011, v. 9, N 4, p. 925-932.
12. H. Mehrer. *Diffusion in solids.* Berlin: Springer, 2007, 651 p.
13. N.A. Azarenkov, V.E. Semenenko, A.I. Ovcharenko, *Proc. VIII School-seminar of Young Scientists «Crystal Growth».* Kharkov, 2014, p. 28.
14. I. Takahashi, N. Usami, K. Kutsukake, et al. Generation mechanism of dislocations during directional solidification of multicrystalline silicon using artificially designed seed // *J. Cryst. Growth.* 2010, v. 312, p. 897-901.
15. С.В. Лєнков, В.В. Зубарев, Д.В. Лукомський, В.В. Видолоб. Дефекти кремнієвих фотоелектричних перетворювачів // *Вісник Київського національного університету ім. Тараса Шевченка:* Військово-спеціальні науки. 2006, №12, с. 19-23.
16. В.Е. Семененко, Н.Н. Пилипенко, В.А. Позняков. Дислокационная структура естественных микрокомпозиционных материалов // *ВАНТ. Серия «Вакуум, чистые материалы, сверхпроводники».* 2009, №6(64), с. 227- 231.
17. N.A. Azarenkov, V.E. Semenenko, A.V. Leonovich, T.A. Kovalenko. Bimonocrystall materials – in situ refractory microcomposites // *Journal of Kharkiv National University. Series «Nuclei, Particles, Fields».* 2013, №1041, issue 2(58), p 111-115.
18. Н.А. Азаренков, В.Е. Семененко, С.В. Литовченко. *Фазовые равновесия и диаграммы состояния.* Харьков: ХНУ им. В.Н. Каразина, 2006, 100 с.
19. Н.В. Немчинова, В.Э. Клёц. Рафинирование металлургического кремния методом зонной плавки // *Физические свойства металлов и сплавов:* Сб. науч. трудов. Екатеринбург: УГТУ-УПИ, 2009, ч. 2, с. 223-227.
20. Н.А. Азаренков, В.Е. Семененко, В.А. Позняков. Высокотемпературные естественные микрокомпозиты // *Металлофизика и новейшие технологии.* 2011, т. 33, №12, с. 379-391.
21. В.А. Макара, Л.П. Стебленко, Н.Я. Горидько и др. О влиянии постоянного магнитного поля на электропластический эффект в кристаллах кремния // *Физика твердого тела*. 2001, т. 43, в. 3, с. 462-465.
22. Н.А. Азаренков, В.Е. Семененко, Н.Г. Стервоедов, А.А. Касилов. Влияние диффузионных процессов на структурную стабильность и износостойкость естественных микрокомпозитов // *ВАНТ. Серия «Физика радиационных повреждений и радиационное материаловедение».* 2011, №2(97), с. 149-154.
23. M.J. Hytch, J.-L. Putaux, J. Thibault. Stress and strain around grain-boundary dislocations measured by

high-resolution electron microscopy // *Philosophical Magazine*. 2006, v. 86, issue 29-31, p. 4641-4656.

24. J. Schmidt, K. Bothe. Structure and transformation of the metastable boron- and oxygen-related defect center in crystalline silicon // *Phys. Rev. B*. 2004, v. 69, p. 024107-1–024107-8.

Article received 01.10.2015

ОСОБЕННОСТИ ОБРАЗОВАНИЯ СОВЕРШЕННОЙ МОНОКРИСТАЛЛИЧЕСКОЙ СТРУКТУРЫ ЛЕГИРОВАННЫХ КРИСТАЛЛОВ КРЕМНИЯ

Н.А. Азаренков, В.Е. Семененко, А.И. Овчаренко, Н.Н. Пилипенко

Изучены особенности выращивания совершенных легированных монокристаллов кремния. Выявлены особенности анодного травления монокристаллов n- и p-типов. Определено влияние ориентации затравок на эволюцию дислокационной и дефектной структур в кристалле на различных стадиях роста. Установлено влияние термообработки на структурно-фазовое состояние монокристаллов и время жизни неравновесных носителей тока.

ОСОБЛИВОСТІ ФОРМУВАННЯ ДОСКОНАЛОЇ МОНОКРИСТАЛІЧНОЇ СТРУКТУРИ ЛЕГОВАНИХ КРИСТАЛІВ КРЕМНІЮ

М.О. Азарєнков, В.Є. Семененко, А.І. Овчаренко, М.М. Пилипенко

Вивчено особливості вирощування досконалих легованих монокристалів кремнію. Виявлено особливості анодного травлення монокристалів n- і p-типів. Визначено вплив орієнтації запалу на еволюцію дислокаційної і дефектної структур у кристалі на різних стадіях росту. Встановлено вплив термообробки на структурно-фазовий стан монокристалів і час життя нерівноважних носіїв струму.